Alkyl Branching Position in Diketopyrrolopyrrole Polymers: Interplay between Fibrillar Morphology and Crystallinity and Their Effect on Photogeneration and Recombination in Bulk-Heterojunction Solar Cells

Shivhare, Rishi; Erdmann, Tim; Hoermann, Ulrich; Collado-Fregoso, Elisa; Zeiske, Stefan; Benduhn, Johannes; Ullbrich, Sascha; Huebner, Rene; Hambsch, Mike; Kiriy, Anton; Voit, Brigitte; Neher, Dieter; VANDEWAL, Koen & Mannsfeld, Stefan C. B. (2018) Alkyl Branching Position in Diketopyrrolopyrrole Polymers: Interplay between Fibrillar Morphology and Crystallinity and Their Effect on Photogeneration and Recombination in Bulk-Heterojunction Solar Cells. In: Chemistry of materials, 30(19), p. 6801-6809.

DOI: 10.1021/acs.chemmater.8b02739
Handle: http://hdl.handle.net/1942/28761

DOI: 10.1002/((Communication, No. aenm.201800451))
Article type: Communication

Impact of Triplet Excited States on the Open-Circuit Voltage of Organic Solar Cells

Johannes Benduhn, Fortunato Piersimoni, Giacomo Londi, Anton Kirch, Johannes Widmer , Christian Koerner , David Beljonne, Dieter Neher, Donato Spoltore, Koen Vandewal**

J. Benduhn, A. Kirch, Dr. J. Widmer[a)], Dr. C. Koerner[b)], Dr. D. Spoltore, Prof. Dr. Vandewal[c)]
Institut für Angewandte Physik, Technische Universität Dresden, Nöthnitzer Str. 61, 01187 Dresden, Germany
E-mail: johannes.benduhn@iapp.de and koen.vandewal@uhasselt.be

Dr. F. Piersimoni, Prof. D. Neher
Institute of Physics and Astronomy, University of Potsdam, Karl-Liebknecht-Str. 24-25, 14476 Potsdam, Germany

G. Londi, Prof. Dr. D. Beljonne
Chimie des Matériaux Nouveaux & Centre d'Innovation et de Recherche en Matériaux Polymères, Université de Mons, Place du Parc 20, 7000 Mons, Belgium

Keywords: organic solar cells, non-radiative voltage losses, triplet excited states, charge-transfer states

ABSTRACT. The best organic solar cells (OSCs) achieve comparable peak external quantum efficiencies (EQE_{PV}) and fill factors (FF) as conventional photovoltaic devices. However, their voltage losses are much higher, in particular those due to non-radiative recombination. To investigate the possible role of triplet states on the donor or acceptor materials in this process, we study model systems comprising Zn- and Cu-phthalocyanine (Pc), as well as fluorinated versions of these donors, combined with C_{60} as acceptor. Fluorination allows us to tune the energy level alignment between the lowest energy triplet state (T_1) and the charge-transfer (CT) state, while the replacement of Zn by Cu as the central metal in the Pcs leads to a largely enhanced spin-orbit coupling. Only in the latter case, we observe a substantial influence of the triplet state on the non-radiative voltage losses. In contrast, we find that for a large series of

[a)] current address: Heliatek GmbH, Treidlerstraße 3, 01139 Dresden, Germany
[b)] current address: Organic Electronics Saxony, Würzburger Str. 51, 01187 Dresden, Germany
[c)] current address: Institute for Materials Research (IMO-IMOMEC), Hasselt University, Wetenschapspark 1, 3590 Diepenbeek, Belgium

typical OSC materials, the relative energy level alignment between T_1 and the CT state does not substantially affect non-radiative voltage losses.

Introduction

In contrast to organic light emitting diodes (OLEDs), organic solar cells (OSCs) are still awaiting a market breakthrough.[1][2][3] A major challenge for OSCs is their relatively low power conversion efficiency (PCE).[4][5] The main reason is their low open-circuit voltage (V_{OC}) as compared to the optical gap (E_{opt}) of the main absorbing materials.[6]

All photovoltaic (PV) technologies suffer from voltage losses, arising from fundamental radiative recombination and parasitic non-radiative recombination. Radiative recombination is inevitable, and is the only recombination process taking place in an ideal solar cell.[7][8][9][10] This process determines the upper limit of the V_{OC}, denoted as the radiative open-circuit voltage V_r. In reality, the measured V_{OC} is lower than V_r due to the presence of non-radiative decay channels, lowering V_r by ΔV_{nr}:

$$\Delta V_{nr} = V_r - V_{OC} \,. \tag{1}$$

Rau has shown that ΔV_{nr} is proportional to the natural logarithm of the quantum efficiency of emission (EQE_{EL}).[7] The validity of Eq. (1) for OSCs has been shown previously,[11][12] where ΔV_{nr} typically accounts for 0.25–0.40 V of the total voltage losses ($\Delta V_{OC} = E_{CT} - V_{OC}$).[12][8][13][14] This is a much higher value than in inorganic and Perovskite solar cells, where $\Delta V_{nr} \leq 0.15$ V.[15][16][17]

In addition to voltage losses due to radiative and non-radiative recombination, OSCs suffer voltage losses because the photo-generated excitons on the donor (D) or acceptor (A) undergo a charge transfer to form an interfacial charge-transfer (CT) state with energy E_{CT}. However, it has been recently shown that the energy difference between the optical gap of the donor or acceptor and the CT state ($E_{opt} - E_{CT}$) can be minimized to less than 0.05 eV [18][13] and even down to 0.01 eV [6], without sacrificing efficient free charge carrier generation. Therefore, in

the OSCs with the currently lowest voltage losses, non-radiative recombination is the main reason for the low V_{OC} as compared to other PV technologies employing absorber with similar optical gaps.

In a previous study, we have shown for a whole range of solution and vacuum processed OSCs that ΔV_{nr} correlates with E_{CT}. This led us to the conclusion that non-radiative decay is mediated by CT state decay via electron-phonon coupling.[12] However, in the related OLED technology, the major non-radiative decay channel is mediated by the triplet excited states.[19] In OSCs, triplet states are present on both the D and A materials, and for high voltage OSCs the energy of the lowest energy triplet state T_1 (E_{T1}) on one or both compounds may be lower than E_{CT}.[20][21][22] Moreover, Chow et. al. reported that recombination via T_1 can drive a large fraction of the overall recombination in OSCs.[23]

In this paper, we therefore investigate under which circumstances, low energy T_1 states affect non-radiative recombination losses and the V_{OC} of OSCs. We study model systems comprising Zn- and Cu-phthalocyanines (ZnPc, CuPc) combined with C_{60} as electron acceptor. Fluorination of the phthalocyanines (Pcs) results in an increase of the CT state energy, lifting it 0.33-0.40 eV above the T_1 state of the donor. Surprisingly, we find that, in contrast to OLEDs, T_1 is not the main responsible for the dominating non-radiative decay in typical OSCs. We generalize this finding by studying a substantial amount of OSCs. Only in the case of a large coupling of T_1 to the ground state, introduced for example by the presence of Cu, non-radiative decay via T_1 significantly contributes to the voltage losses.

Determination of E_{T1} for the Metal-Phthalocyanine Donors

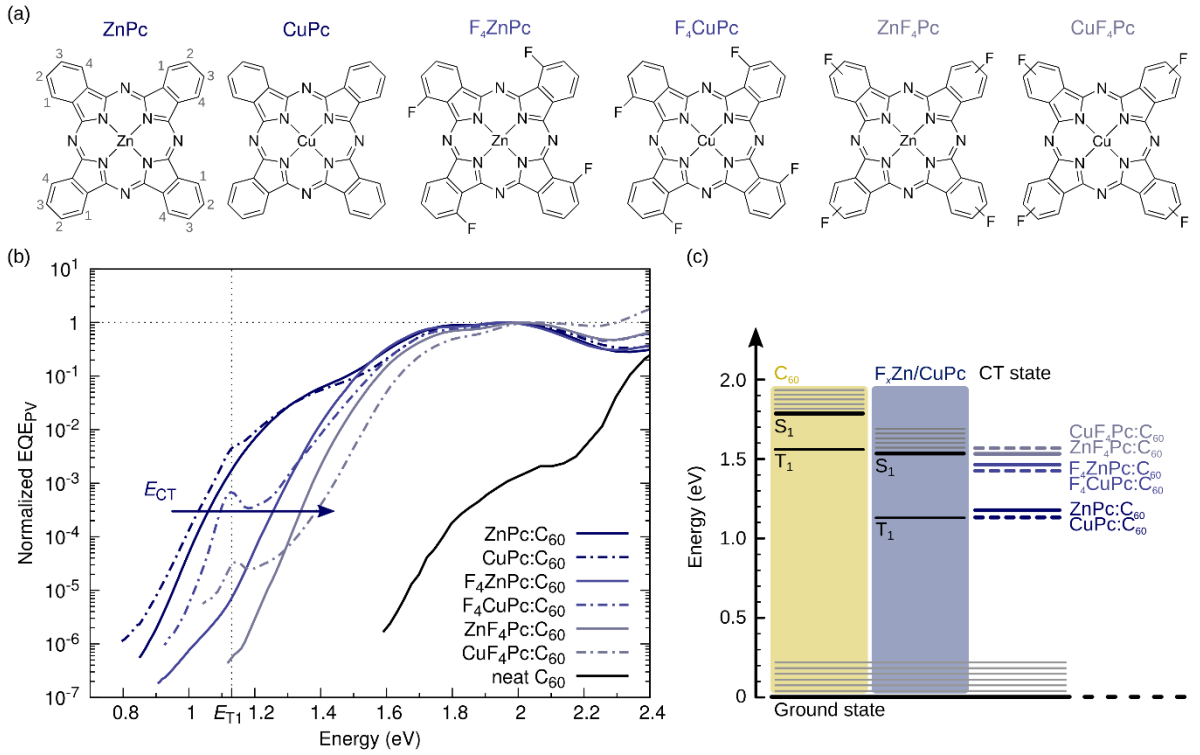

Figure 1. a) Molecular structures of the donor molecules and their short names used throughout the manuscript. In the molecular structure of ZnPc, the free bonding positions at the benzene ring are numbered. For the donors ZnF_4Pc and CuF_4Pc, fluorine binds either to position (2) or (3) of the corresponding benzene ring. **b)** Normalized sensitive EQE_{PV} spectra as a function of the photonenergy for OSCs comprising the above shown donor molecules and C_{60} as acceptor. The ZnPc series is shown with solid blue lines. The CuPc series, represented by dash-dot blue lines, shows distinct photocurrent feature at 1.13 eV, related to triplet absorption. **c)** Shows the corresponding energy levels of the pure absorbers and the corresponding CT state.

To investigate the impact of T_1 on ΔV_{nr}, we chose suitable model systems comprising the donors ZnPc, CuPc, and their fluorinated derivatives. See **Figure 1**a for the molecular structures. These donors are co-evaporated with C_{60} as acceptor and used as absorber in OSCs. Fluorination increases E_{CT}, while the minimum singlet (S_1) excitation energy E_{S1} remains

relatively invariant. Employing Cu as a central metal atom is an elegant way to precisely obtain E_{T1}. Indeed, optical transitions from and to the triplet manifold of Pcs containing Cu are possible due to the fact that Cu has an unpaired $4s^1$ electron in the standard electron configuration, mediating a spin flip.[24][25] When comparing OSCs employing C_{60} as acceptor and either ZnPc or CuPc as donor molecules, we notice for CuPc indeed an additional absorption feature at 1.13 eV, see Figure 1b.[26] This additional absorption appears at the same position in OSCs with fluorinated derivatives of CuPc. Moreover, we find for these OSCs electroluminescence (EL) peaks at similar photon energies, see Figure S2 and S3 in the supporting information (SI). This additional absorption and emission is not visible in any of the ZnPc based devices and has been directly linked to the enhanced coupling of T_1 to the ground state in CuPc, mediated by the unpaired $4s^1$ electron.[24][25][27] Therefore, we obtain E_{T1} = 1.13 eV from the crossing point of reduced EQE_{PV} and EL spectra of F_4CuPc and CuF_4Pc, see Figure S3 in the SI. Since the wavefunction of T_1 of metal-Pc is mainly located on the organic ligand, the Pc, we expect that the E_{T1} values for ZnPc and its fluorinations are very similar to E_{T1} of the CuPc compounds. In order to shed some light on the nature of the low-energy electronic transitions and assess their energies and oscillator strengths, we performed highly correlated complete active space self-consistent field (CASSCF) calculations. These indicate that E_{S1} and E_{T1} vary only weakly with chemical structure across the series of compounds investigated (see Table S4 in the SI). Most importantly, the calculated oscillator strength of T_1 for Cu-based Pc's is 150-800 fold higher than that of the Zn-based molecules. More details of the calculations can be found in the SI. Results from Vincett and co-workers confirm the value of E_{T1} which we obtained, by directly observing phosphorescence of CuPc and ZnPc in solution at 77 K, with a peak energy of 1.16 eV and 1.13 eV, respectively.[27] Moreover, thin films of CuPc, measured at room temperature, showed photoluminescence at a peak position of E = 1.12-1.13 eV, further confirming the obtained E_{T1} in our thin films.[28][29][30]

Fluorination of Donor Molecule Increases E_{CT} and V_{OC}

When fluorinating ZnPc or CuPc, the energy of the highest occupied molecular orbital (HOMO) and the lowest unoccupied molecular orbital (LUMO) shifts away from the vacuum level simultaneously,[31] resulting in a similar E_{S1} for all donor molecules, see Figure S1a in the SI. In the first type of fluorination (F_4-metal-Pc), all 4 fluorine atoms are attached only to equivalent positions (1) or (4) of the outer benzene ring. In the second case, denoted metal-F_4Pc, the 4 fluorine atoms can be attached randomly either to position (2) or (3) of the benzene ring, which is schematically sketched in Figure 1a. All these configurations of metal-F_4Pc are chemically and energetically very similar and not distinguishable.

Table 1. Information on the OSC performance of the metal-Pc:C_{60} series.

Donor	j_{SC}[d)] [mA/cm²]	FF[d)] [%]	PCE[d)] [%]	V_{OC}[d)] [V]	V_r[e)] [V]	E_{CT}[f)] [eV]	V_0[g)] [V]	E_{CT} - qV_0 [eV]
ZnPc	8.1	59.4	2.7	0.56	0.94	1.17	1.10 ± 0.02	0.07 ± 0.02
CuPc	6.9	49.0	1.6	0.48	0.91	1.13	1.05 ± 0.01	0.08 ± 0.01
F_4ZnPc	7.3	58.1	3.1	0.73	1.12	1.46*	1.31 ± 0.02	0.15 ± 0.02
F_4CuPc	2.4	41.0	0.6	0.61	1.02	1.42*	1.17 ± 0.01	0.25 ± 0.01
ZnF_4Pc	2.2	33.1	0.6	0.89	1.21	1.53*	1.43 ± 0.02	0.10 ± 0.02
CuF_4Pc	0.5	29.4	0.1	0.75	1.21	1.56*	1.48 ± 0.01	0.08 ± 0.01

[d)] The listed performance values correspond to a mismatch corrected illumination with simulated sunlight at an intensity of 1000 Wm^{-2}.

[e)] V_r was calculated from the EQE_{PV} and EL spectra, assuming the reciprocity relation between absorption and emission.[7][8]

[f)] E_{CT} was obtained from Gaussian fit to the EQE_{PV} and EL spectra following Ref. [8]. If denoted with *, E_{CT} was obtained from the crossing point between EQE_{PV} and EL, for more information see Figure S2 in the SI.

[g)] V_0 represents the V_{OC} extrapolated to 0 K and was obtained from temperature dependent *j-V* curves at different illumination intensities. The denoted V_0 represents the mean value for 7 different illumination intensities and the statistical error of the mean value.

E_{CT} of the OSCs is obtained from sensitive EQE_{PV} and EL spectra as outlined earlier.[8] The values of E_{CT} are listed in **Table 1**, more details on the determination procedure can be found in Figure S2 in the SI. As shown in Figure 1b and 1c, fluorination leads to shifted positions of the HOMO and LUMO of the donor molecules, resulting in an increased E_{CT}. While T_1 is clearly the lowest energy state for the fluorinated Pcs, V_{OC} still correlates with E_{CT} rather than E_{T1}, for both the Zn- and Cu- containing blends. We discuss this in more detail in the next paragraphs.

Enhanced Coupling of T_1 to Ground State Increases Voltage Losses

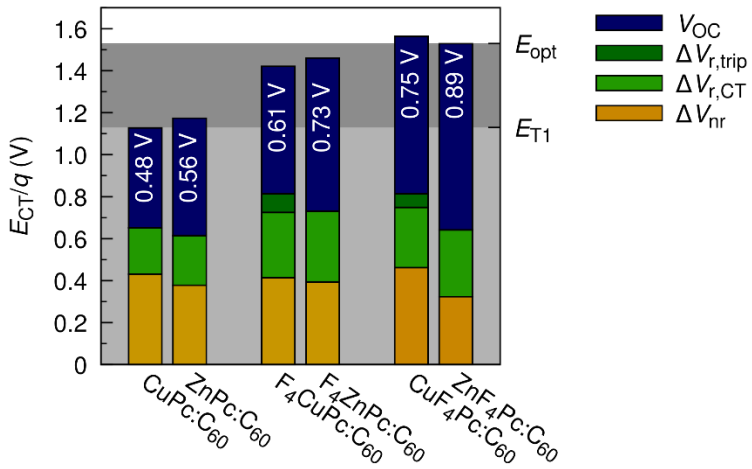

Figure 2. Detailed representation of the voltage losses in the series of OSCs consisting of the metal-Pc donor series and C_{60} as acceptor. The dark grey area represents E_{opt} of the donor and the light grey area highlights the donor's E_{T1}. The height of the full column represents E_{CT}, divided by the elementary charge q. The dark blue column represents the measured V_{OC}. The green bar represents the fundamental radiative voltage losses, and the yellow bar the non-radiative voltage losses, which were obtained by taking the difference between the calculated V_r and the measured V_{OC}. For the OSCs comprising F_4CuPc and CuF_4Pc, the increased coupling of the triplet-doublet to the ground state causes additional voltage losses due to radiative triplet state decay, shown as a dark green bar.

The bar diagram in **Figure 2** summarizes the energetic situation and voltage losses for the 6 different OSCs. The height of each bar depicts E_{CT} of the corresponding device. The V_{OC} is reduced as compared to E_{CT} due to fundamental radiative voltage losses (ΔV_r, shown in light green), and parasitic non-radiative voltage losses (ΔV_{nr}, shown in yellow). Radiative and non-radiative voltage losses are calculated from the sensitively measured EQE_{PV} and EL spectra, following the method outlined in ref. [8]. Additional ΔV_r caused by radiative decay of T_1 are obtained from the difference between the V_r values calculated with and without considering the absorption of T_1 (highlighted in dark green). The optical gap (E_{opt}) of the device corresponds to the E_{S1} of the donor, being at ~1.53 eV, since it is lower than that of C_{60}.

Within each of the 3 pairs of donor molecules containing either Zn or Cu (non-fluorinated and two differently fluorinated metal-Pc's) E_{CT} is very comparable. However, V_{OC} is always significantly lower for devices containing Cu as compared to Zn. The E_{CT} of CuPc:C_{60} is about 0.04 eV smaller than that of ZnPc:C_{60}, but the V_{OC} for CuPc:C_{60} is about 0.08 V lower because ΔV_{nr} is increased by 0.05 V and ΔV_r is slightly decreased. When fluorinating CuPc to F_4CuPc, E_{CT} increases and, as compared to CuPc, the voltage losses E_{CT}/q - V_{OC} increase drastically. Here, T_1 is the lowest energy level in the system and due to the substantial oscillator strength of the T_1-to-ground-state transition, the total radiative recombination increases and consequently reduces the V_{OC}. The radiative character of the additional recombination, introduced by T_1, in the F_4CuPc:C_{60} device can be seen in the EL spectra in Figure S2 in the SI. In CuPc:C_{60} the radiative recombination is instead mediated by the CT state. Indeed, for the F_4ZnPc device, voltage losses E_{CT}/q - V_{OC} are 0.08 V smaller as compared to F_4CuPc, which can be fully attributed to the absence of radiative losses through T_1. In the OSCs containing ZnF_4Pc and CuF_4Pc, the voltage losses for the CuF_4Pc based device are even more pronounced and ΔV_{nr} and ΔV_r are both significantly higher as compared to ZnF_4Pc.

When comparing the overall performance of the OSCs, it's immediately clear that, although the films absorb a similar amount of light (see Figure S1b in the SI), the j_{SC} and FF for Cu

containing OSCs are always lower than for the Zn containing ones, especially when $E_{T1} < E_{CT}$ (case of F_4CuPc and CuF$_4$Pc). This indicates an increased coupling of T_1 in the Cu containing compounds, harmful for charge generation and extraction. However, details of the charge generation and extraction processes in this series of compounds are beyond the scope of this paper.

Impact of T_1 on the Low-Temperature Limit of V_{OC}

To understand the possible impacts of T_1 on the voltage losses in more detail, we analyzed basic recombination rate equations, c.f. Figure S5 in the SI. In the case that E_{T1} is lower than E_{CT}, we deduce 3 important cases:

(i) When *T_1 states repopulate the CT state faster than decaying but its decay rate is higher than direct CT state decay,* all excited states are in equilibrium and in the limit of $T \rightarrow 0$ K, V_{OC} approaches E_{T1}.

(ii) When *T_1 decays faster or similarly fast than T_1 dissociation into CT states,* then T_1 states are not in equilibrium with CT states and free carriers, causing extra recombination losses via T_1 population and decay. In the limit of $T \rightarrow 0$ K, V_{OC} approaches E_{CT}.

(iii) When *recombination via the CT state is faster than the population and decay of T_1*, the impact of T_1 is negligible. In the limit of $T \rightarrow 0$ K, V_{OC} approaches E_{CT}.

Temperature dependent *j-V* curves performed at different light intensities allow us to determine which particular case applies to a certain device. From extrapolation of V_{OC} to $T \rightarrow 0$ K, V_0 is obtained and compared to E_{T1} and E_{CT}. The experimental data is shown in Figure S4 in the SI and the values are listed in Table 1 for each device. For all OSCs where the splitting between T_1 and E_{CT} is relatively small (ZnPc, CuPc) and for the donors F_4ZnPc and ZnF$_4$Pc, we find $V_0 \approx E_{CT}$, with V_0 being slightly (~0.10 eV) lower than E_{CT}. This indicates that even if T_1 is the lowest energy state, it does not affect V_0 when the coupling of T_1 to ground state is

indeed small (case (ii) or (iii)). The slightly lower V_0 than E_{CT} is due to the fact that E_{CT} slightly decreases upon cooling as reported in Ref. [8][32]. However, for F_4CuPc, we observe $V_0 \approx E_{T1}$, located 0.25 eV below E_{CT}. This indicates that T_1, the CT state, and the free charge carriers are in equilibrium and that the recombination to the ground state is mediated by T_1 (case (i)). For CuF_4Pc, we find that $V_0 \approx E_{CT} \approx E_{opt}$. Here, recombination involves the S_1 state in this OSC and V_0 corresponds to E_{opt}. For this configuration T_1 just adds recombination losses for $T > 0$ K (case (ii)).

In summary, we find that if T_1 is lower than E_{CT} and if its coupling to the ground state is high, e.g. the case of F_4CuPc, it significantly increases the total voltage losses ΔV_{OC} (case (i)) as compared to the normal case, where the T_1-ground-state coupling is much weaker (e.g. F_4ZnPc). Only in the latter case V_{OC} is expected to correlate with E_{CT} independently from the exact position of the lower laying T_1. However, it is still unclear if in this case, T_1 causes additional ΔV_{nr}. Therefore, we investigate ΔV_{nr} for a series of archetypical OSC materials including cases where E_{T1} is higher and lower than E_{CT}.

Insensitivity of Non-Radiative Voltage Losses on E_{T1}

For commonly used OSC materials the determination of E_{T1} is difficult due to the fact that optical transitions between T_1 and the ground state are forbidden. In the literature, several alternative approaches have been reported to obtain E_{T1}. Local T_1 states always have a lower energy than S_1 because of the exchange energy of the antibonding spin state, which is usually assumed not be larger than 1eV.[33][19][34][35][36] One method to obtain E_{T1} is to circumvent the low electronic coupling of T_1 to the ground state by substituting heavy atoms and thereby enhancing the phosphorescence. E_{T1} is then assumed to be similar in energy as for the original molecule.[19] Another indirect way is to use a host-guest system, in which the quenching of the emission of a series of guest molecules can provide an estimation of the relative energetic

position of T_1.[19][36] Alternatively, density functional theory calculations have been used to predict E_{T1}, but uncertainties of the absolute value are often rather large.

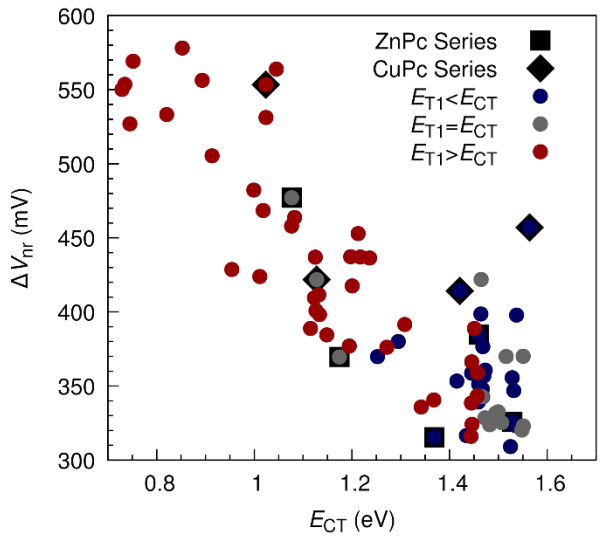

Figure 3. Comparison of ΔV_{nr} for several OSCs with either $E_{T1} > E_{CT}$ or $E_{T1} < E_{CT}$ indicated by blue or red filled circles, respectively. Since determination of E_{T1} is difficult, grey filled circles represent OSCs where published values present an uncertainty of $E_{T1} - E_{CT} \leq \pm 100$ meV. The black squares and diamonds indicate the investigated series of OSCs employing non-fluorinated and fluorinated ZnPcs and CuPcs as donor, respectively. Details on the shown OSCs can be found in the SI.

In **Figure 3**, we compare ΔV_{nr} for a large set of OSCs, distinguishing different relative alignments of T_1 and the CT state. The ΔV_{nr} values were partly published in Ref. [12] and are re-analyzed for this paper. The investigated devices comprise vacuum deposited small molecules in planar and bulk heterojunction architecture[12][37][38][39] and solution processed polymers.[8][11][40][41][42] We performed an intensive literature study to obtain the lowest energy E_{T1} of either donor or acceptor, via one of the methods described above, see Table S1 in SI for details.[40][43][44][45][46][40][47][48][49][50][51][52][53][54][55][56][57][58] We compare E_{T1} to the E_{CT} obtained from sensitive EQE_{PV} spectra.[8][12] OSCs where $E_{T1} < E_{CT}$ are represented by blue dots.

Devices where $E_{T1} > E_{CT}$ are shown by red dots. As outlined above, the determination of E_{T1} has a significant uncertainty and, therefore, all OSCs where we find $E_{T1} - E_{CT} \leq \pm 100$ meV are represented by the grey dots.

In contrast to fluorescent OLED materials, where T_1 drives non-radiative recombination[19][20], we find that in general, low energy T_1 states do not necessarily affect ΔV_{nr} in OSCs. The summarizing Figure 3 shows several devices around $E_{CT} = 1.5$ eV which have similarly low ΔV_{nr} independently whether E_{T1} is above or below E_{CT}. Furthermore, for devices with the highest ΔV_{nr}, T_1 is actually higher in energy than E_{CT}. As previously reported, ΔV_{nr} depends on the absolute value of E_{CT}, rather than on the $E_{T1} - E_{CT}$ difference. The exception to this finding are the CuPc and fluorinated CuPc samples, discussed above, which are indicated with black diamonds in Figure 3.

In conclusion, we find that only in the cases with enhanced coupling to the ground state, T_1 limits the V_{OC} and drives most of the recombination. However, in the most common cases, using small organic molecules or polymers, we find that the energetic position of E_{T1} as compared to E_{CT} is of secondary importance in determining ΔV_{nr} and the overall V_{OC} losses of OSCs. Studies aiming at understanding and reducing ΔV_{nr} should instead focus on non-radiative CT state decay, even in the high voltage, low energy loss case where local triplet states are the lowest energy excited states.

Experimental Section

Device preparation: The layers of the OSCs of the Metal-Phthalocyanine series are thermally evaporated at ultra-high vacuum (base pressure < 10^{-7} mbar) on a glass substrate with a pre-structured ITO contact (Thin Film Devices, USA). For an appropriate electron contact 15 nm of n-C_{60}, doped with $Cr_2(hpp)_4$ (Novaled GmbH, Germany) at 3 wt%, are deposited and followed by the active layer comprising 30 nm of donor molecule (ZnPc (zinc-phthalocyanine, CreaPhys GmbH, Germany) or CuPc (copper-phthalocyanine, abcr GmbH, Germany) or F_4ZnPc (tetrafluoro-zinc-phthalocyanine, BASF, Germany) or F_4CuPc (tetrafluoro-copper-phthalocyanine, synthesized by M.L.) or ZnF_4Pc (tetrafluoro-zinc-phthalocyanine or synthesized by B.B.) or CuF_4Pc (tetrafluoro-copper-phthalocyanine, synthesized by B.B.) co-evaporated with C_{60} (CreaPhys GmbH, Germany) at a 1:1 weight ratio. Afterwards, 5 nm of an intrinsic hole transport layer (HTL) (BF-DPB (*N,N′*-diphenyl-*N,N′*-bis(9,9-dimethyl-fluoren-2-yl)-benzidine, Synthon Chemicals GmbH, Germany) or BPAPF (9,9-bis[4-(*N,N*-bis-biphenyl-4-yl-amino)phenyl]-9*H*-fluorene, Lumtec, Taiwan)) and 40 nm of p-doped HTL (BF-DPB with 10 wt% NPD9 and BPAPF with 5 wt% NDP9; NDP9 is a p-dopant supplied by Novaled GmbH, Germany). The OSC is finished with 100 nm of Al. All the organic materials were purified 2-3 times by sublimation. The device is defined by the geometrical overlap of the bottom and the top contact and equals 6.44 mm^2. To avoid exposure to ambient conditions, the organic part of the device was covered by a small glass substrate which is glued on top.

Current-voltage characteristics are measured with a SMU (Keithley 2400, USA) at standard testing conditions (16 S-150 V.3 Solar Light Co., USA) with a mismatch (mismatch = 0.62…0.76) corrected light intensity.

Temperature dependent current-voltage measurements: For temperature variation, the sample is mounted onto a temperature controlled copper block in vacuum, differences due to a temperature gradient in the substrate between temperature sensor (Type K thermocouple) and the active sample area are corrected by prior calibration. The systematic error for the

temperature is estimated be smaller than 5 K. The sample is illuminated by a white light LED. The V_{OC} is measured with a source measure unit. It is interpolated from the two points of the current–voltage characteristic where the sign of the current density changes.

Sensitive EQE$_{PV}$ measurements: The light of a quartz halogen lamp (50 W) is chopped at 140 Hz and coupled into a monochromator (Newport Cornerstone 260 1/4m, USA). The resulting monochromatic light is focused onto the OSC, its current at short-circuit conditions is fed to a current pre-amplifier before it is analyzed with a lock-in amplifier (Signal Recovery 7280 DSP, USA). The time constant of the lock-in amplifier was chosen to be 1 s and the amplification of the pre-amplifier was increased to resolve low photocurrents. The EQE_{PV} is determined by dividing the photocurrent of the OSC by the flux of incoming photons, which was obtained with a calibrated silicon (Si) and indium-gallium-arsenide (InGaAs) photodiode.

Electroluminescence measurements were obtained with an Andor SR393i-B spectrometer equipped with a cooled Si and cooled InGaAs detector array (DU420A-BR-DD and DU491A-1.7, UK). The spectral response of the setup was calibrated with a reference lamp (Oriel 63355). The emission spectrum of the OSCs was recorded at different injection currents, which correspond to applied voltages lower than or at least similar to the V_{OC} of the device at 1 sun illumination.

Computational details: The ground-state geometric structure of the donor compounds was optimized at the Density Functional Theory level with the calculation's suite Gaussian 16.[59] The HSE06 exchange-correlation functional was used,[60] as in a previous work.[61] The 6-31G(d,p) basis set was employed for non-metallic atoms, while a larger one was chosen for Cu and Zn, namely AUG-cc-pVTZ. The D_{4h} symmetry point group was imposed throughout the geometry optimization process. Then, CASSCF calculations were carried out on the optimized structures with the ORCA 4.0.1 suite.[62] A Def2-TZVPP basis set was used, along with the RIJCOSX approximation to speed up the calculations. An N-Electron Valence State Perturbation Theory (NEVPT2) approach, as implemented in the ORCA code, was introduced

in order to correct the CASSCF energies for dynamic correlation effects. At last, spin-orbit coupling (SOC) relativistic effects were added to refine the NEVPT2 transition energies and assess the associated oscillator strengths.

Supporting Information
Supporting Information is available from the Wiley Online Library or from the author.

Acknowledgements
This work was supported by the German Federal Ministry for Education and Research (BMBF) through the InnoProfile project "Organische p-i-n Bauelemente 2.2" and the European Union's Horizon 2020 research and innovation programme under Marie Sklodowska Curie grant agreement No.722651 (SEPOMO). F.P. and D.N. acknowledge funding by the German Research Foundation (DFG) via the SFB 951 "HIOS". We acknowledge Prof. K. Leo and V. C. Nikolis for fruitful discussions. We thank Dr. B. Beyer for supplying ZnF_4Pc and CuF_4Pc as well as Dr. M. Lau for the synthesis of F_4CuPc. Additionally, we thank Prof. Bäuerle from University of Ulm for the supply of DH4T, DH6T and several DCV_2-nT-R. Furthermore, we acknowledge Felix Holzmueller, Matthias Saalfrank, and Rico Meerheim for providing OSC devices for this study. Computational resources were provided by the Consortium des Équipements de Calcul Intensif (CÉCI), funded by the Fonds de la Recherche Scientifiques de Belgique (F.R.S.-FNRS) under Grant No. 2.5020.11, as well as the Tier-1 supercomputer of the Fédération Wallonie-Bruxelles, infrastructure funded by the Walloon Region under Grant Agreement No. 1117545. D.B. is a FNRS Research Director.

Received: ((will be filled in by the editorial staff))
Revised: ((will be filled in by the editorial staff))
Published online: ((will be filled in by the editorial staff))

References

[1] K. Leo, *Nat. Rev. Mater.* **2016**, *1*, 16056.

[2] J. E. Carlé and F. C. Krebs, *Sol. Energy Mater. Sol. Cells* **2013**, *119*, 309.

[3] S. B. Darling and F. You, *RSC Adv.* **2013**, *3*, 17633.

[4] K. Leo, *Nat. Nanotechnol.* **2015**, *10*, 574.

[5] M. A. Green, K. Emery, Y. Hishikawa, W. Warta, E. D. Dunlop, D. H. Levi and A. W. Y. Ho-Baillie, *Prog. Photovolt.* **2017**, *25*, 659.

[6] V. C. Nikolis, J. Benduhn, F. Holzmueller, F. Piersimoni, M. Lau, O. Zeika, D. Neher, C. Koerner, D. Spoltore and K. Vandewal, *Adv. Energy Mater.* **2017**, 1700855.

[7] U. Rau, *Phys. Rev. B* **2007**, *76*, 085303.

[8] K. Vandewal, K. Tvingstedt, A. Gadisa, O. Inganäs and J. V. Manca, *Phys. Rev. B* **2010**, *81*, 125204.

[9] W. Shockley and H. J. Queisser, *Journal of Applied Physics* **1961**, *32*, 510.

[10] H. J. Queisser, *Materials Science and Engineering: B* **2009**, *159-160*, 322.

[11] K. Vandewal, K. Tvingstedt, A. Gadisa, O. Inganäs and J. V. Manca, *Nat. Mater.* **2009**, *8*, 904.

[12] J. Benduhn, K. Tvingstedt, F. Piersimoni, S. Ullbrich, Y. Fan, M. Tropiano, K. A. McGarry, O. Zeika, M. K. Riede, C. J. Douglas, S. Barlow, S. R. Marder, D. Neher, D. Spoltore and K. Vandewal, *Nat. Energy* **2017**, *2*, 17053.

[13] K. Vandewal, Z. F. Ma, J. Bergqvist, Z. Tang, E. G. Wang, P. Henriksson, K. Tvingstedt, M. R. Andersson, F. L. Zhang and O. Inganäs, *Adv. Funct. Mater.* **2012**, *22*, 3480.

[14] J. Yao, T. Kirchartz, M. S. Vezie, M. a. Faist, W. Gong, Z. He, H. Wu, J. Troughton, T. Watson, D. Bryant and J. Nelson, *Phys. Rev. Appl.* **2015**, *4*, 014020.

[15] M. A. Green, *Prog. Photovoltaics* **2012**, *20*, 472.

[16] K. Tvingstedt, O. Malinkiewicz, A. Baumann, C. Deibel, H. J. Snaith, V. Dyakonov and H. J. Bolink, *Sci. Rep.* **2014**, *4*, 06071.

[17] W. Tress, *Adv. Energy Mater.* **2017**, 1602358.

[18] N. A. Ran, J. A. Love, C. J. Takacs, A. Sadhanala, J. K. Beavers, S. D. Collins, Y. Huang, M. Wang, R. H. Friend, G. C. Bazan and T. Q. Nguyen, *Adv. Mater.* **2016**, *28*, 1482.

[19] A. Köhler and H. Bässler, *Mat. Sc. Eng. R* **2009**, *66*, 71.

[20] A. Rao, P. C. Y. Chow, S. Gelinas, C. W. Schlenker, C.-Z. Li, H.-L. Yip, A. K.-Y. Jen, D. S. Ginger and R. H. Friend, *Nat.* **2013**, *500*, 12339.

[21] F. Etzold, I. A. Howard, N. Forler, A. Melnyk, D. Andrienko, M. R. Hansen and F. Laquai, *Energy Environ. Sci.* **2015**, *8*, 1511.

[22] D. W. Gehrig, I. A. Howard and F. Laquai, *J. Phys. Chem. C* **2015**, *119*, 13509.

[23] P. C. Y. Chow, S. Gélinas, A. Rao, R. H. Friend, S. Gélinas, A. Rao and R. H. Friend, *J. Am. Chem. Soc.* **2014**, *136*, 3424.

[24] M. G. Cory and M. C. Zerner, *Chem. Rev.* **1991**, *91*, 813.

[25] I. Bruder, J. Schöneboom, R. Dinnebier, A. Ojala, S. Schäfer, R. Sens, P. Erk and J. Weis, *Org. Electron.* **2010**, *11*, 377.

[26] F. Piersimoni, D. Cheyns, K. Vandewal, J. V. Manca and B. P. Rand, *J. Phys. Chem. Lett.* **2012**, *3*, 2064.

[27] P. S. Vincett, E. M. Voigt and K. E. Rieckhoff, *J. Chem. Phys.* **1971**, *55*, 4131.

[28] W. Y. Tong, H. Y. Chen, A. B. Djurišić, A. M. Ng, H. Wang, S. Gwo and W. K. Chan, *Opt. Mater.* **2010**, *32*, 924.

[29] A. G. Kazanski, E. I. Terukov, A. V. Ziminov, O. B. Gusev, A. V. Fenukhin, A. G. Kolosko, I. N. Trapeznikova, Y. A. Nikolaev and B. Modu, *Tech. Phys. Lett.* **2005**, *31*, 782.

[30] A. V. Fenukhin, A. G. Kazanskii, A. G. Kolosko, E. I. Terukov and A. V. Ziminov, *J. Non-Cryst. Solids* **2006**, *352*, 1668.

[31] T. Mayer, U. Weiler, C. Kelting, D. Schlettwein, S. Makarov, D. Wöhrle, O. Abdallah, M. Kunst and W. Jaegermann, *Sol Energ Mat Sol C* **2007**, *91*, 1873.

[32] T. M. Burke, S. Sweetnam, K. Vandewal and M. D. McGehee, *Adv. Energy Mater*. **2015**, *5*, 1500123.

[33] H. Uoyama, K. Goushi, K. Shizu, H. Nomura and C. Adachi, *Nat.* **2012**, *492*, 234.

[34] A. Köhler, J. S. Wilson, R. H. Friend, M. K. Al-Suti, M. S. Khan, A. Gerhard and H. Bässler, *J. Chem. Phys.* **2002**, *116*, 9457.

[35] A. Köhler and D. Beljonne, *Adv. Funct. Mater.* **2004**, *14*, 11.

[36] A. P. Monkman, H. D. d. G. M. M. Burrows, I. Hamblett and S. Navaratnam, *Chem. Phys. Lett.* **1999**, *307*, 303.

[37] T. Moench, P. Friederich, F. Holzmueller, B. Rutkowski, J. Benduhn, T. Strunk, C. Koerner, K. Vandewal, A. Czyrska-Filemonowicz, W. Wenzel and K. Leo, *Adv. Energy Mater.* **2016**, *6*, 1501280.

[38] R. Fitzner, E. Mena-Osteritz, A. Mishra, G. Schulz, E. Reinold, M. Weil, C. Koerner, H. Ziehlke, C. Elschner, K. Leo, M. Riede, M. Pfeiffer, C. Uhrich and P. Bäuerle, *J. Am. Chem. Soc.* **2012**, *134*, 11064.

[39] C. Koerner, C. Elschner, N. C. Miller, R. Fitzner, F. Selzer, E. Reinold, P. Bäuerle, M. F. Toney, M. D. McGehee, K. Leo and M. Riede, *Org. Electron.* **2012**, *13*, 623.

[40] E. T. Hoke, K. Vandewal, J. A. Bartelt, W. R. Mateker, J. D. Douglas, R. Noriega, K. R. Graham, J. M. J. Fréchet, A. Salleo and M. D. Mcgehee, *Adv. Energy Mater.* **2013**, *3*, 220.

[41] K. Vandewal, A. Gadisa, W. D. Oosterbaan, S. Bertho, F. Banishoeib, I. Van Severen, L. Lutsen, T. J. Cleij, D. Vanderzande and J. V. Manca, *Adv. Funct. Mater.* **2008**, *18*, 2064.

[42] K. Vandewal, W. D. Oosterbaan, S. Bertho, V. Vrindts, A. Gadisa, L. Lutsen, D. Vanderzande and J. V. Manca, *Appl. Phys. Lett* **2009**, *95*, 21.

[43] J. W. Arbogast, A. P. Darmanyan, C. S. Foote, Y. Rubin, F. N. Diederich, M. M. Alvarez, S. J. Anz and R. L. Whetten, *J. Phys. Chem* **1991**, *95*, 11.

[44] D. Beljonne, J. Cornil, R. H. Friend, R. A. J. Janssen and J. L. Brédas, *J. Am. Chem. Soc.* **1996**, *118*, 6453.

[45] D. Di Nuzzo, A. Aguirre, M. Shahid, V. S. Gevaerts, S. C. J. Meskers and R. A. J. Janssen, *Adv. Mater.* **2010**, *22*, 4321.

[46] K. Goushi, K. Yoshida, K. Sato and C. Adachi, *Nat. Photon.* **2012**, *6*, 253.

[47] R. R. Hung and J. J. Grabowski, *J. Phys. Chem.* **1991**, *95*, 6073.

[48] D. K. K. Liu and L. R. Faulkner, *J. Am. Chem. Soc.* **1977**, *99*, 4594.

[49] K. Sato, K. Shizu, K. Yoshimura, A. Kawada, H. Miyazaki and C. Adachi, *Phys. Rev. Lett.* **2013**, *110*, 247401.

[50] R. Schueppel, K. Schmidt, C. Uhrich, K. Schulze, D. Wynands, J. L. Brédas, E. Brier, E. Reinold, H.-B. Bu, P. Baeuerle, B. Maennig, M. Pfeiffer and K. Leo, *Phys. Rev. B* **2008**, *77*, 85311.

[51] J. S. Swensen, E. Polikarpov, A. Von Ruden, L. Wang, L. S. Sapochak and A. B. Padmaperuma, *Adv. Funct. Mater.* **2011**, *21*, 3250.

[52] D. Veldman, S. C. J. Meskers and R. A. J. Janssen, *Adv. Funct. Mater.* **2009**, *19*, 1939.

[53] M. R. Wasielewski, M. P. O'Neil, K. R. Lykke, M. J. Pellin and D. M. Gruen, *J. Am. Chem. Soc.* **1991**, *113*, 2774.

[54] R. M. Williams, J. M. Zwier and J. W. Verhoeven, *J. Am. Chem. Soc.* **1995**, *117*, 4093.

[55] B. Xu and S. Holdcroft, *Adv. Mater.* **1994**, *6*, 325.

[56] C. Murawski, C. Fuchs, S. Hofmann, K. Leo and M. C. Gather, *Appl. Phys. Lett.* **2014**, *105*, 113303.

[57] I. Lim, E.-K. Kim, S. A. Patil, D. Y. Ahn, W. Lee, N. K. Shrestha, J. K. Lee, W. K. Seok, C.-G. Cho and S.-H. Han, *RSC Adv.* **2015**, *5*, 55321.

[58] S. Pfuetzner, A. Petrich, C. Malbrich, J. Meiss, M. Koch, M. K. Riede, M. Pfeiffer and K. Leo, *Proc. SPIE 6999 Organic Optoelectronics and Photonics III*, **2008**, 69991M

[59] M. J. Frisch, G. W. Trucks, H. B. Schlegel, G. E. Scuseria, M. A. Robb, J. R. Cheeseman, G. Scalmani, V. Barone, G. A. Petersson, H. Nakatsuji, X. Li, M. Caricato, A. V. Marenich, J. Bloino, B. G. Janesko, R. Gomperts, B. Mennucci, H. P. Hratchian, J. V. Ortiz, A. F. Izmaylov, J. L. Sonnenberg, D. Williams-Young, F. Ding, F. Lipparini, F. Egidi, J. Goings, B. Peng, A. Petrone, T. Henderson, D. Ranasinghe, V. G. Zakrzewski, J. Gao, N. Rega, G. Zheng, W. Liang, M. Hada, M. Ehara, K. Toyota, R. Fukuda, J. Hasegawa, M. Ishida, T. Nakajima, Y. Honda, O. Kitao, H. Nakai, T. Vreven, K. Throssell, J. J. A. Montgomery, J. E. Peralta, F. Ogliaro, M. J. Bearpark, J. J. Heyd, E. N. Brothers, K. N. Kudin, V. N. Staroverov, T. A. Keith, R. Kobayashi, J. Normand, K. Raghavachari, A. P. Rendell, J. C. Burant, S. S. Iyengar, J. Tomasi, M. Cossi, J. M.

Millam, M. Klene, C. Adamo, R. Cammi, J. W. Ochterski, R. L. Martin, K. Morokuma, O. Farkas, J. B. Foresman and D. J. Fox, "Gaussian 16 Revision A.03," **2016**.

[60] J. Heyd and G. E. Scuseria, *J. Chem. Phys.* **2004**, *121*, 1187.

[61] N. Marom, O. Hod, G. E. Scuseria and L. Kronik, *J. Chem. Phys.* **2008**, *128*.

[62] F. Neese, *Wires. Comput. Mol. Sc.* **2012**, *2*, 73.